

TNCT-0601

Spin polarization and chiral symmetry breaking at finite density

Shinji Maedan ¹

*Department of Physics, Tokyo National College of Technology, Kunugida-machi,
Hachioji, Tokyo 193-0997, Japan*

Abstract

We investigate the possibility of the spin polarization of quarks at zero temperature and moderate baryon density. The Nambu-Jona-Lasinio (NJL) model including interactions in vector and axial-vector channel is used, and the self consistent equations for the spin polarization and chiral condensate are solved numerically in the framework of the Hartree approximation. We find that the interplay between the spin polarization and the chiral symmetry plays an important role. If the chemical potential of quarks reaches a certain finite value, the spin polarization begins to occur because the quark still has relatively large dynamical mass, which is generated by spontaneous chiral symmetry breaking. On the other hand, when the spin polarization occurs, it operates to lower the dynamical quark mass a little. When one increases the chemical potential furthermore, the spin polarization becomes weaker and finally disappears because the dynamical quark mass is fairly reduced by restoring partially the chiral symmetry.

¹E-mail: maedan@tokyo-ct.ac.jp

1 Introduction

The density of matter in cores of neutron stars is of order $O(10^{15}\text{g/cm}^3)$, and the neutron star will give us useful information on how the matter behaves with very high density. In neutron stars, it is supposed that nuclear matter or quark matter exists. One of the distinctive features of the neutron star is that it has a strong magnetic field $O(10^{12}\text{Gauss})$. In order to explain the origin of the strong magnetic field in neutron stars, the possibility of the spin polarization in nuclear matter has been studied by many authors [1]; however, no definite conclusion has been obtained. Recently, instead of nuclear matter, several authors investigate the possibility of the spin polarization in quark matter [2, 3], which is expressed by axial vector $\langle\bar{\psi}\gamma_5\gamma\psi\rangle = \langle\psi^\dagger\Sigma\psi\rangle$ with Σ being the spin operator of the quark in the relativistic quantum field theory[4]. This article is one of such investigations. We consider the possibility of the spin polarization of quarks at zero temperature and moderate baryon density at which asymptotic freedom of quarks does not hold. In such a density region, the interplay between the spin polarization and spontaneous chiral symmetry breaking of QCD will be important.

QCD describes the dynamics of quarks and gluons. For the study of neutron stars with high baryon density, one needs to understand the properties of QCD at finite density, which have been investigated vigorously by use of effective theories of QCD [5]. At low temperature and low density, quarks and gluons are confined and chiral symmetry is broken spontaneously, while at low temperature and high density, deconfinement occurs and chiral symmetry will be restored, furthermore a new phase called color superconductivity may be realized [6, 7]. In Ref.[3], a coexistent phase of spin polarization and color superconductivity in high-density QCD is investigated. The authors of Ref.[3] use the one-gluon-exchange interaction as an effective interaction between quarks, which implies that the density is taken to be high so that one can treat the coupling constant $\alpha_s = g^2/4\pi$ very small. The quark mass is treated as the constant parameter not depending on the density, and the numerical calculations are carried out for several different values of the quark mass. It is shown that the spin polarization remarkably depends on the value of the quark mass. Especially, the spin polarization does not occur in the limit of zero quark mass, which is shown analytically by use of the self consistent equation in the framework of the mean field approximation [3].

In this paper, we investigate the possibility of the spin polarization of quarks at zero temperature and moderate baryon density, at which spontaneous symmetry breaking of chiral symmetry plays an important role. When the quark number density increases, the quark mass can not be regarded as a constant, because the chiral symmetry is gradually restored and the dynamical quark mass decreases [8, 9]. How the spin polarization is influenced by the dynamical quark mass which decreases due to restoration of chiral symmetry? Conversely, how the dynamical quark mass is influenced by occurrence of the spin polarization? The point we concentrate is the interplay between the spin polarization and chiral symmetry. Although the relation between the chiral symmetry

breaking phase and the color superconducting phase has been discussed [10], we do not consider the color superconductivity in the present paper and focus on the relation between chiral symmetry and the spin polarization.

The method of our approach is as follows. Since the color gauge coupling constant is not small at the moderate density, one can not use the one-gluon-exchange interaction as an effective interaction between quarks. Instead, effective theories of QCD such as the Nambu-Jona-Lasinio (NJL) model [11] are often used at that moderate density region. The NJL model realizes spontaneous symmetry breaking of chiral symmetry while it does not confine quarks; nevertheless the properties of mesons can be well described by the NJL model [9]. The model we use is the NJL type model including interactions in vector and axial-vector channel as well as scalar and pseudoscalar channel, which model is used to deal with (axial) vector meson modes [12, 13, 9].

The paper is organized as follows. The model we use is described in the next section and the chemical potential μ of quarks is introduced so as to deal with the system with finite density. Using the Hartree approximation (the mean field approximation), we can obtain the propagator of the quark in the presence of the mean fields of chiral condensate, quark number density, and axial-vector field. In section 3, the self consistent equations for chiral condensate, quark number density, and axial-vector field related to the spin polarization are derived respectively in the framework of the mean field approximation. These simultaneous self consistent equations are solved numerically in section 4. The results of the numerical calculations tell us how the spin polarization arises or how the dynamical quark mass changes as the chemical potential of quarks is varied. Section 5 is devoted to conclusion.

2 Formulation and the Hartree approximation

In this section, the model we use is introduced. Assuming the presence of the mean fields of chiral condensate, $\langle\bar{\psi}\psi\rangle$, quark number density, $\langle\bar{\psi}\gamma^0\psi\rangle$, and axial-vector, $\langle\bar{\psi}\gamma_5\gamma^3\psi\rangle$, at finite density, we calculate the propagator of the quark in the Hartree approximation.

The following NJL type model [9] with the number of colors $N_c = 3$ and the number of flavors $N_f = 1$ is used,

$$\mathcal{L} = \mathcal{L}_0 + \mathcal{L}_S + \mathcal{L}_V, \quad (1)$$

$$\begin{aligned} \mathcal{L}_0 &= \bar{\psi}(i\partial - m)\psi, \\ \mathcal{L}_S &= \frac{G_1}{2} \left[(\bar{\psi}\psi)^2 + (\bar{\psi}i\gamma_5\psi)^2 \right], \\ \mathcal{L}_V &= -\frac{G_2}{2} \left[(\bar{\psi}\gamma_\mu\psi)(\bar{\psi}\gamma^\mu\psi) + (\bar{\psi}\gamma_\mu\gamma_5\psi)(\bar{\psi}\gamma^\mu\gamma_5\psi) \right]. \end{aligned}$$

The vector and axial-vector interaction term \mathcal{L}_V is needed for treatment of vector meson or axial-vector meson in the NJL type model. This lagrangian is chiral invariant if the

current quark mass m is zero. We make use of this lagrangian in order to investigate the interplay between the spin polarization and chiral symmetry, and regard coupling constants G_1 and G_2 as free parameters.

The chemical potential μ of quarks is introduced to treat the system with finite density, $\mathcal{L} + \mu \bar{\psi} \gamma^0 \psi$. Now, we suppose that the following mean fields exist at finite density,

$$\langle \bar{\psi} \psi \rangle, \quad \langle \bar{\psi} \gamma^0 \psi \rangle, \quad \langle \bar{\psi} \gamma_5 \gamma^3 \psi \rangle, \quad (2)$$

where $\langle \bar{\psi} \gamma_5 \gamma_3 \psi \rangle = \langle \psi^\dagger \Sigma_z \psi \rangle$ is an expectation value of the z -component of the quark's spin Σ ; one can choose the z -component as the direction of the spin polarization without loss of generality. In the vacuum state ($\mu = 0$), chiral symmetry is broken spontaneously, $\langle \bar{\psi} \psi \rangle \neq 0$, and no spin polarization occurs, $\langle \bar{\psi} \gamma_5 \gamma^3 \psi \rangle = 0$. As noted in the previous section, color superconductivity is not considered in this paper. Using the Hartree approximation (mean field approximation), we obtain the lagrangian with bilinear form,

$$\begin{aligned} \mathcal{L}_{\text{MF}} = & \bar{\psi} (i\partial - m) \psi + G_1 \langle \bar{\psi} \psi \rangle \bar{\psi} \psi - G_2 \langle \bar{\psi} \gamma^0 \psi \rangle \bar{\psi} \gamma^0 \psi + G_2 \langle \bar{\psi} \gamma_5 \gamma^3 \psi \rangle \bar{\psi} \gamma_5 \gamma^3 \psi \\ & + \mu \bar{\psi} \gamma^0 \psi \\ \equiv & \bar{\psi}_\alpha^c (G_A^{-1})_{\alpha\beta}^{cc'} \psi_\beta^{c'}, \end{aligned} \quad (3)$$

where $\alpha, \beta = 1, 2, 3, 4$ are the spinor indices, and $c, c' = 1, 2, 3$ are the color indices. The G_A^{-1} is rewritten more compact form as

$$\begin{aligned} (G_A^{-1})_{\alpha\beta}^{cc'} = & \left[i\partial - m + G_1 \langle \bar{\psi} \psi \rangle + \left\{ \mu - G_2 \langle \bar{\psi} \gamma^0 \psi \rangle \right\} \gamma^0 + G_2 \langle \bar{\psi} \gamma_5 \gamma^3 \psi \rangle \gamma_5 \gamma^3 \right]_{\alpha\beta} (\mathbf{1})^{cc'} \\ \equiv & \left[i\partial - M + \mu_r \gamma^0 + U_A \gamma_5 \gamma^3 \right]_{\alpha\beta} (\mathbf{1})^{cc'}, \end{aligned} \quad (4)$$

with

$$\begin{aligned} M & \equiv m - G_1 \langle \bar{\psi} \psi \rangle, \\ \mu_r & \equiv \mu - G_2 \langle \bar{\psi} \gamma^0 \psi \rangle, \\ U_A & \equiv G_2 \langle \bar{\psi} \gamma_5 \gamma^3 \psi \rangle. \end{aligned} \quad (5)$$

The chemical potential μ is shifted to $\mu - G_2 \langle \bar{\psi} \gamma^0 \psi \rangle$ in G_A^{-1} . In momentum space,

$$\begin{aligned} G_A^{-1} = & \left[\not{q} + \mu_r \gamma^0 - M + U_A \gamma_5 \gamma^3 \right] (\mathbf{1}) \\ \equiv & \left[\not{p} - M + U_A \gamma_5 \gamma^3 \right] (\mathbf{1}), \end{aligned} \quad (6)$$

with

$$p^\mu = (p_0, \mathbf{p}) \equiv (q_0 + \mu_r, \mathbf{q}). \quad (7)$$

The quark propagator G_A ($G_A G_A^{-1} = 1$) is obtained as (see Appendix A)

$$G_A = (\mathbf{1}) \left[\not{p} - M + U_A \gamma_5 \gamma^3 \right]^{-1}$$

$$\begin{aligned}
&= (1) \frac{1}{(p^2 - M^2 - U_A^2)^2 - 4 U_A^2 (M^2 + p_z^2)} \\
&\quad \times \left[(p^2 - M^2 + U_A^2) M + (p^2 - M^2 - U_A^2) \not{p} - 2 U_A^2 p_z (\gamma^3) \right. \\
&\quad + 2 U_A p_z p_\mu (\gamma_5 \gamma^\mu) - U_A (p^2 + M^2 - U_A^2) (\gamma_5 \gamma^3) \\
&\quad \left. + 2 U_A M (p_0 \sigma^{12} - p_x \sigma^{02} + p_y \sigma^{01}) \right]. \tag{8}
\end{aligned}$$

The propagator G_A has four energy poles [3], $p_0 = \epsilon_n$ ($n = 1, 2, 3, 4$),

$$\begin{aligned}
\epsilon_1 = \epsilon_- &= \sqrt{p_\perp^2 + \left(\sqrt{M^2 + p_z^2} - U_A \right)^2}, \\
\epsilon_2 = \epsilon_+ &= \sqrt{p_\perp^2 + \left(\sqrt{M^2 + p_z^2} + U_A \right)^2}, \\
\epsilon_3 &= -\epsilon_1, \\
\epsilon_4 &= -\epsilon_2, \tag{9}
\end{aligned}$$

where $p_\perp^2 = p_x^2 + p_y^2$ and $\epsilon_{1,2}$ represents positive energy while $\epsilon_{3,4}$ represents negative energy. Peculiarities of the Fermi surface of ϵ_n are described in detail in Ref.[3]

3 Self consistent equation

In this section, we derive self consistent equations in the framework of the mean field approximation, each of which can be calculated analytically in the zero temperature limit. These self consistent equations will be solved numerically in the next section. The self consistent equations for $\langle \bar{\psi} \psi \rangle$, $\langle \bar{\psi} \gamma^0 \psi \rangle$, and $\langle \bar{\psi} \gamma_5 \gamma^3 \psi \rangle$ are expressed with the quark propagator G_A , respectively,

$$\langle \bar{\psi} \psi \rangle = -i \text{Tr}\{G_A\}, \tag{10}$$

$$\langle \bar{\psi} \gamma^0 \psi \rangle = -i \text{Tr}\{G_A \gamma^0\}, \tag{11}$$

$$\langle \bar{\psi} \gamma_5 \gamma^3 \psi \rangle = -i \text{Tr}\{G_A \gamma_5 \gamma^3\}. \tag{12}$$

They are rewritten in terms of M , μ , and U_A that are introduced in Eq.(5),

$$M = m + i G_1 \text{Tr}\{G_A\}, \tag{13}$$

$$\mu_r = \mu + i G_2 \text{Tr}\{G_A \gamma^0\}, \tag{14}$$

$$U_A = -i G_2 \text{Tr}\{G_A \gamma_5 \gamma^3\}. \tag{15}$$

These three equations are simultaneous equations for three unknowns, namely the dynamical quark mass M , the "shifted" quark chemical potential μ_r , and the spin polarization U_A .

3.1 Self consistent equation for M .

When the system with finite temperature T is concerned, one can employ the imaginary time formulation [14, 15], according to which the q_0 in the propagator Eq.(8) is replaced by the Matsubara frequency, $i\omega_j = i(2j+1)\pi T$, ($j \in \mathbf{Z}$). Let us begin with the calculation of $\text{Tr}\{G_A\}$ in the self consistent equation for M , Eq.(13). In the imaginary time formulation, one needs to perform the Matsubara sum over $q_0 = i\omega_j$,

$$\begin{aligned}\text{Tr}\{G_A\} &= \int \frac{d^3q}{(2\pi)^3} \left(i T \sum_{j=-\infty}^{\infty} \right) \text{tr}\{G_A\} \\ &= \int \frac{d^3p}{(2\pi)^3} \left(i T \sum_{j=-\infty}^{\infty} \right) N_c \frac{4 M(p^2 - M^2 + U_A^2)}{(p^2 - M^2 - U_A^2)^2 - 4 U_A^2 (M^2 + p_z^2)},\end{aligned}\quad (16)$$

where $p_0 = q_0 + \mu_r = i\omega_j + \mu_r$. The result of the sum is (see Appendix B)

$$\text{Tr}\{G_A\} = i N_c \int \frac{d^3p}{(2\pi)^3} \left[\sum_{n=1,2,3,4} \frac{M \left\{ \sqrt{M^2 + p_z^2} + (-1)^n U_A \right\}}{\epsilon_n \sqrt{M^2 + p_z^2}} \tilde{f}(\epsilon_n - \mu_r) \right], \quad (17)$$

where $\tilde{f}(\epsilon_n - \mu_r) \equiv 1/\{e^{\beta(\epsilon_n - \mu_r)} + 1\}$ is the Fermi-distribution ($\beta = 1/T$). In the zero temperature limit $T \rightarrow 0$, the self consistent equation for M then becomes

$$\begin{aligned}M &= m - G_1 N_c \int \frac{d^3p}{(2\pi)^3} \left[\sum_{n=1,2} \frac{M \left\{ \sqrt{M^2 + p_z^2} + (-1)^n U_A \right\}}{\epsilon_n \sqrt{M^2 + p_z^2}} \theta(\mu_r - \epsilon_n) \right. \\ &\quad \left. + \sum_{n=3,4} \frac{M \left\{ \sqrt{M^2 + p_z^2} + (-1)^n U_A \right\}}{\epsilon_n \sqrt{M^2 + p_z^2}} \theta(\sqrt{\Lambda^2 + M^2} - |\epsilon_n|) \right].\end{aligned}\quad (18)$$

Since the terms coming from the negative energy ($\epsilon_{3,4} < 0$) contribution in Eq.(17) diverge in the zero temperature limit, we regularize these terms by $\theta(\sqrt{\Lambda^2 + M^2} - |\epsilon_n|)$ in Eq.(18) with cutoff Λ .

3.2 Self consistent equations for μ_r , U_A .

First, the self consistent equation for μ_r , Eq.(14), is calculated. As the $\text{Tr}\{G_A\}$ in Eq.(13), $\text{Tr}\{G_A\gamma^0\}$ is calculated as follows,

$$\text{Tr}\{G_A\gamma^0\} = i N_c \int \frac{d^3p}{(2\pi)^3} \left[\sum_{n=1,2,3,4} \tilde{f}(\epsilon_n - \mu_r) - 2 \right]. \quad (19)$$

The self consistent equation for μ_r is then

$$\mu_r = \mu - G_2 N_c \int \frac{d^3p}{(2\pi)^3} \sum_{n=1,2} \theta(\mu_r - \epsilon_n), \quad (20)$$

in the zero temperature limit $T \rightarrow 0$.

Secondly, the self consistent equation for U_A , Eq.(15), is considered. $\text{Tr}\{G_A\gamma_5\gamma^3\}$ is evaluated as

$$\text{Tr}\{G_A\gamma_5\gamma^3\} = -i N_c \int \frac{d^3 p}{(2\pi)^3} \left[\sum_{n=1,2,3,4} \frac{\{U_A + (-1)^n \sqrt{M^2 + p_z^2}\}}{\epsilon_n} \tilde{f}(\epsilon_n - \mu_r) \right], \quad (21)$$

and in the limit $T \rightarrow 0$, it becomes [3]

$$\begin{aligned} \text{Tr}\{G_A\gamma_5\gamma^3\} = -i N_c \int \frac{d^3 p}{(2\pi)^3} & \left[\sum_{n=1,2} \frac{\{U_A + (-1)^n \sqrt{M^2 + p_z^2}\}}{\epsilon_n} \theta(\mu_r - \epsilon_n) \right. \\ & \left. + \sum_{n=3,4} \frac{\{U_A + (-1)^n \sqrt{M^2 + p_z^2}\}}{\epsilon_n} \right], \end{aligned} \quad (22)$$

where the second term in the right-hand side represents the contribution of the Dirac sea ($\epsilon_{3,4} < 0$). Here, we define the spin polarization of the vacuum state $\mu = 0$ ($\mu_r = 0$) to be zero by subtracting as follows,

$$U_A = -i G_2 \left[\text{Tr}\{G_A\gamma_5\gamma^3\} - \text{Tr}\{G_A\gamma_5\gamma^3\}|_{\mu_r=0} \right], \quad (23)$$

the definition implies that the contribution of the Dirac sea to the spin polarization is neglected. The self consistent equation for U_A eventually takes the form

$$U_A = -G_2 N_c \int \frac{d^3 p}{(2\pi)^3} \sum_{n=1,2} \frac{\{U_A + (-1)^n \sqrt{M^2 + p_z^2}\}}{\epsilon_n} \theta(\mu_r - \epsilon_n), \quad (24)$$

in the zero temperature limit.

We finally obtained the self consistent equations for the dynamical quark mass M , Eq.(18), the "shifted" quark chemical potential μ_r , Eq.(20), and the spin polarization U_A , Eq.(24), in the zero temperature limit. Each of three equations can be calculated analytically if $0 \leq U_A < M$, and the results are shown in Appendix C.

4 Numerical calculations

In this chapter, the numerical solutions for the three self consistent equations Eq.(18), (20), and (24) are obtained, by which we can know how the quark spin polarization U_A or the dynamical quark mass M behaves as the quark chemical potential μ varies. Giving the five input parameters (G_1 , G_2 , m , Λ , μ), we solve these simultaneous equations of three unknowns (M , μ_r , U_A).

At the beginning, let us fix the input parameters. Since we are interested in investigating the relationship between the spin polarization and spontaneous symmetry breaking of the chiral symmetry by use of the NJL model, the G_1 and G_2 are regarded as free parameters. In other words, the pion decay constant or the vector meson mass calculated by our model with these input parameters does not necessarily fit the experimental data. In the vacuum state $\mu = 0$, it becomes $U_A = 0 = \mu_r$, and the value of the effective quark mass (dynamical mass) M_0 in the vacuum state is determined by the current quark mass m , the coupling constant G_1 , and the cutoff Λ . We choose these values as follows,

$$m = 5 \text{ MeV}, \quad G_1 = 0.95 \times 10^{-5} \text{ MeV}^{-2}, \quad \Lambda = 900 \text{ MeV}, \quad (25)$$

by which the self consistent equation Eq.(18) gives the value $M_0 = 316 \text{ MeV}$.

4.1 Numerical results

All the numerical calculations are carried out with the input values of m , G_1 , and Λ given in Eq.(25). The value of G_2 is chosen as $7 \times 10^{-5} \text{ MeV}^{-2}$ in this subsection 4.1, and in the later subsection 4.3, another value $6 \times 10^{-5} \text{ MeV}^{-2}$ of G_2 is chosen.

At first, with the value $G_2 = 7 \times 10^{-5} \text{ MeV}^{-2}$, the self consistent equations, Eq.(18), (20), and (24) are solved numerically. We find that the spin polarization U_A has the nontrivial solution in a chemical potential range of about 350 MeV to 600 MeV, and the numerical results are shown in Fig.1 and Fig.2. In Fig.1, the dynamical quark mass M decreases when the chemical potential μ increases, namely the chiral symmetry is gradually restored as the matter density rises. This graph has the peculiarity; the line of the graph is lowered in the range $350 \text{ MeV} \lesssim \mu \lesssim 600 \text{ MeV}$, which peculiarity will be discussed later. In Fig.2, the nontrivial solution of U_A is figured, and one finds that the quark spin polarization occurs in the chemical potential range $350 \text{ MeV} \lesssim \mu \lesssim 600 \text{ MeV}$. It is notable that the spin polarization disappears when the chemical potential becomes too large, $\mu \gtrsim 600 \text{ MeV}$. This point will be also discussed in the later subsection.

4.2 Effect of the spin polarization U_A on the dynamical quark mass M , and vice versa.

We have solved numerically the simultaneous self consistent equations for M , μ_r , and U_A . The behavior of the dynamical mass M in Fig.1 is influenced by the spin polarization U_A , and the behavior of U_A in Fig.2 is influenced by the dynamical mass M . First, let us consider the effect of the spin polarization U_A on the dynamical mass M . As mentioned before, the behavior of M in Fig.1 has the peculiarity that the line of the graph is lowered in the range $350 \text{ MeV} \lesssim \mu \lesssim 600 \text{ MeV}$. This peculiarity will be caused by the influence of the spin polarization U_A being non-zero in that range of

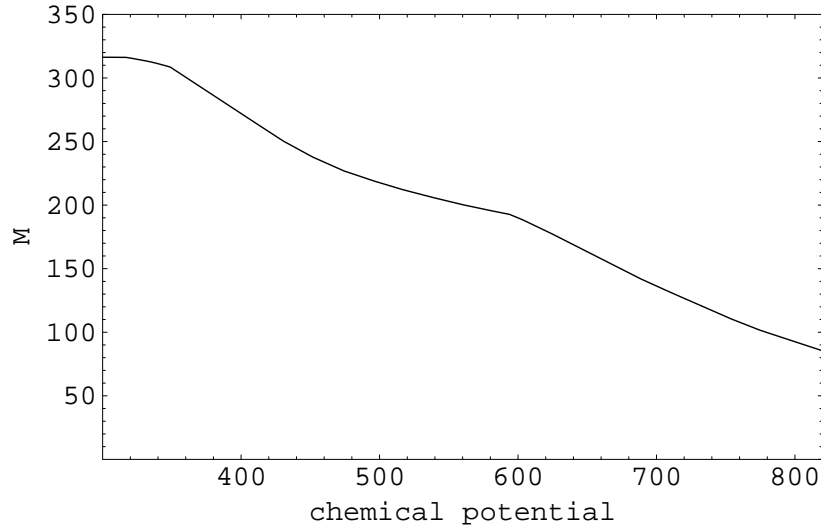


Figure 1: Dynamical quark mass M (MeV) as a function of the chemical potential μ (MeV). The coupling constant is taken to be $G_2 = 7 \times 10^{-5} \text{ MeV}^{-2}$. The M in Fig.1 and the nontrivial solution U_A in Fig.2 are the solution of the simultaneous equations Eq.(18), Eq.(20), and Eq.(24).

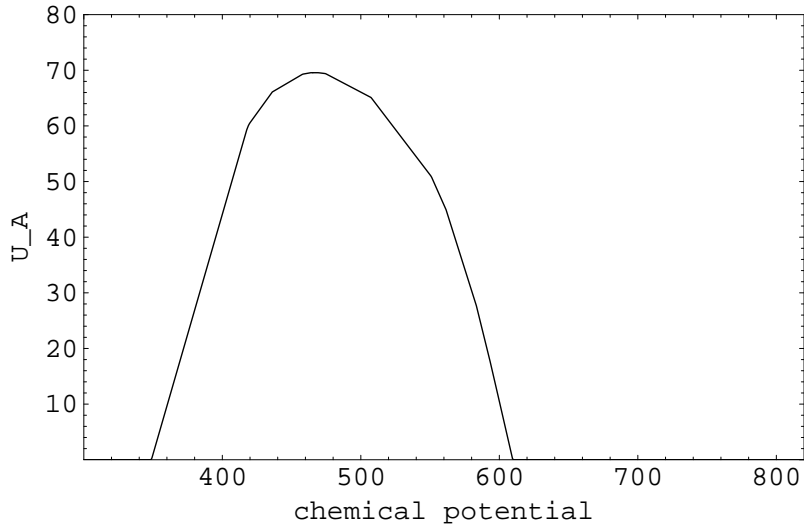


Figure 2: Spin polarization U_A (MeV) as a function of the chemical potential μ (MeV). The coupling constant is taken to be $G_2 = 7 \times 10^{-5} \text{ MeV}^{-2}$. The M in Fig.1 and the nontrivial solution U_A in Fig.2 are the solution of the simultaneous equations Eq.(18), Eq.(20), and Eq.(24).

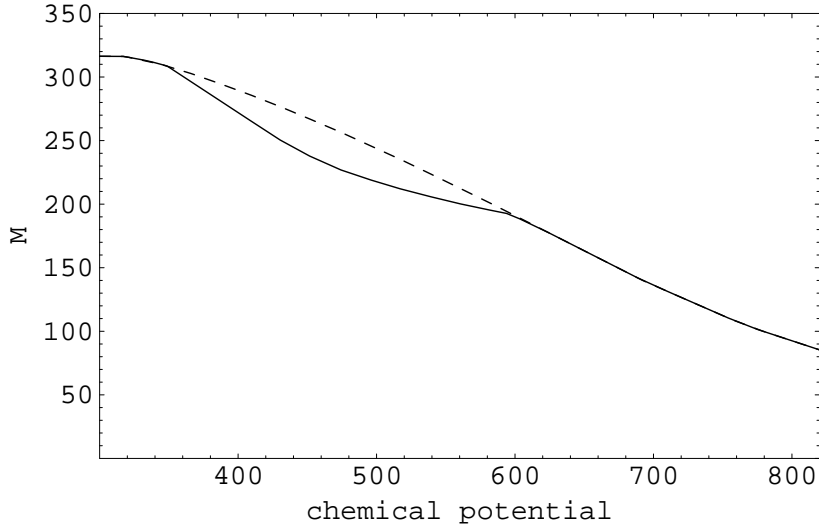


Figure 3: Dynamical quark mass M (MeV) as a function of the chemical potential μ (MeV). The coupling constant is taken to be $G_2 = 7 \times 10^{-5} \text{ MeV}^{-2}$. The dotted line represents the dynamical mass when there is no spin polarization ($U_A = 0$). The solid line represents the dynamical mass with the nontrivial solution U_A (the same result shown in Fig.1).

μ as seen in Fig.2. In order to confirm this, we solve numerically the self consistent equation for M and that for μ_r with setting $U_A = 0$ in the whole range of μ , $0 \leq \mu \leq \Lambda$. The numerical result is shown with the dotted line in Fig.3, and the graph of Fig.1 is also shown in Fig.3 with the solid line for comparison. When the solid line is compared with the dotted line in Fig.3, we find that if the quark spin polarization occurs $U_A > 0$, it operates to lower the dynamical quark mass M which is generated by spontaneous symmetry breakdown of chiral symmetry.

Next, let us consider the effect of the dynamical mass M on the spin polarization U_A . As seen in Fig.1, M is a monotone decreasing function of μ , which passes through a point $(\mu, M) = (469 \text{ MeV}, 229 \text{ MeV})$. As mentioned before, the behavior of U_A in Fig.2 has the peculiarity that the spin polarization U_A disappears when the chemical potential becomes too large, $\mu \gtrsim 600 \text{ MeV}$. This peculiarity may be caused by the fact that the dynamical mass M is the monotone decreasing function of μ . In order to confirm this, we examine how the U_A behaves when the M is taken to be a constant. Specifically speaking, we solve numerically the self consistent equation for U_A and that for μ_r with setting $M = \text{constant} = 229 \text{ MeV}$ ² in the range of $\mu \geq 469 \text{ MeV}$. The numerical result is shown with the dotted line in Fig.4, which shows that the spin polarization U_A becomes larger as μ increases even in the range of large $\mu \gtrsim 600 \text{ MeV}$ if the M is constant (229 MeV). In Fig.4, a part of the graph of Fig.2 ($\mu \geq 469 \text{ MeV}$) is also

²The $M = \text{constant} = 229 \text{ MeV}$ is not a solution of the self consistent equation for M .

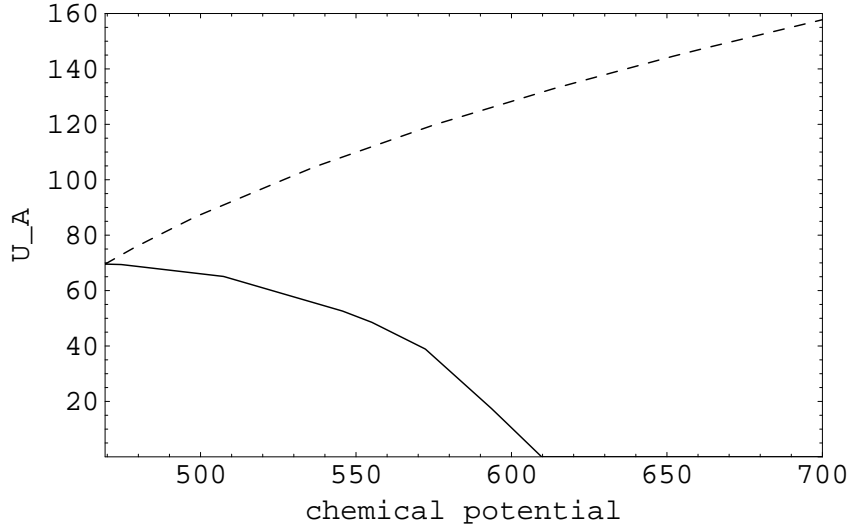


Figure 4: Spin polarization U_A (MeV) as a function of the chemical potential μ (MeV). The coupling constant is taken to be $G_2 = 7 \times 10^{-5} \text{ MeV}^{-2}$. The solid line is a part ($\mu \geq 469$ MeV) of the nontrivial solution shown in Fig.2. The dotted line is obtained when we set the dynamical mass $M = \text{constant} = 229$ MeV.

shown with the solid line. By comparing this solid line with the dotted line in Fig.4, we find that, when the chiral symmetry is gradually restored as the chemical potential μ increases ($\mu \geq 469$ MeV), the dynamical quark mass M reduces ($M \leq 229$ MeV, see Fig.1) and this reduction operates to suppress the spin polarization U_A (see the solid line in Fig.4).

4.3 The case of smaller G_2 value

In order to investigate the effect of the coupling constant G_2 to the spin polarization U_A , we shall do the numerical calculations with the value $G_2 = 6 \times 10^{-5} \text{ MeV}^{-2}$ instead of $G_2 = 7 \times 10^{-5} \text{ MeV}^{-2}$ studied in the previous subsection. In Fig.5, the dotted line represents the case of $G_2 = 6 \times 10^{-5} \text{ MeV}^{-2}$, and the solid line represents the former case of $G_2 = 7 \times 10^{-5} \text{ MeV}^{-2}$ already shown in Fig.2. One can see that the region of the chemical potential μ where the spin polarization occurs $U_A > 0$ becomes narrow when the coupling constant G_2 becomes small. We also plot the spin expectation value per quark in Fig.6, where the dotted line shows the case of $G_2 = 6 \times 10^{-5} \text{ MeV}^{-2}$ and the solid line $G_2 = 7 \times 10^{-5} \text{ MeV}^{-2}$. The spin expectation value per quark

$$-\frac{\langle \psi^\dagger \Sigma_z \psi \rangle}{\langle \psi^\dagger \psi \rangle} = \frac{\langle \bar{\psi} \gamma_5 \gamma^3 \psi \rangle}{\langle \bar{\psi} \gamma^0 \psi \rangle} = \frac{\left(\frac{U_A}{G_2}\right)}{\rho}, \quad (26)$$

equals zero if no spin polarization occurs, and it equals one if all the quarks are com-

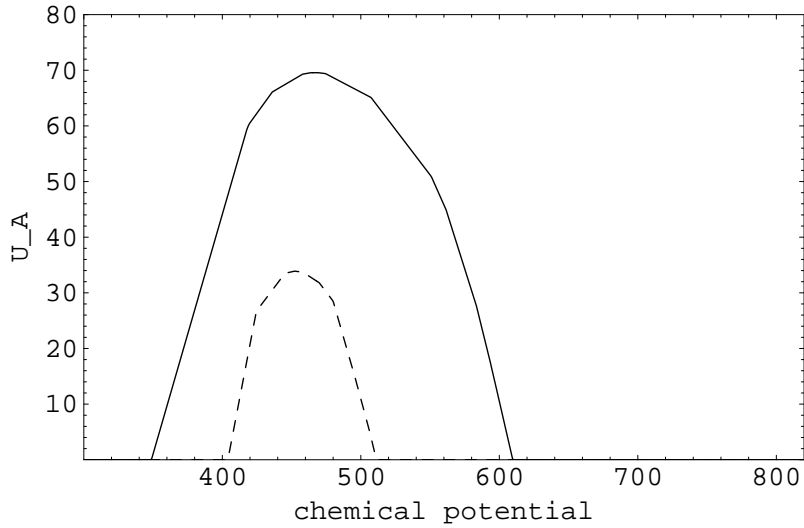


Figure 5: Spin polarization U_A (MeV) as a function of the chemical potential μ (MeV). The solid line is the same result shown in Fig.2 with $G_2 = 7 \times 10^{-5} \text{ MeV}^{-2}$. The dotted line is the result with $G_2 = 6 \times 10^{-5} \text{ MeV}^{-2}$.

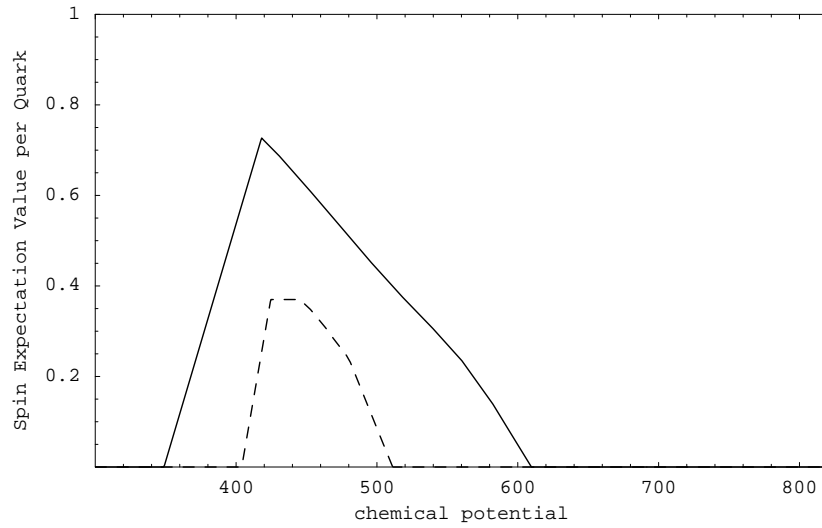


Figure 6: Spin expectation value per quark Eq.(26) as a function of the chemical potential μ (MeV). The solid line is the result with $G_2 = 7 \times 10^{-5} \text{ MeV}^{-2}$. The dotted line is the result with $G_2 = 6 \times 10^{-5} \text{ MeV}^{-2}$.

pletely polarized. The Fig.6 shows that the spin expectation value per quark becomes small when the coupling constant G_2 becomes small.

How does the spin polarization U_A develop when G_2 becomes smaller? With the value of G_2 considerably smaller than $6 \times 10^{-5} \text{ MeV}^{-2}$, say, $1.8 \times 10^{-5} \text{ MeV}^{-2}$, the spin polarization does not take place in the whole range $0 < \mu \leq \Lambda$ with the current quark mass $m = 5 \text{ MeV}$. With such small value $G_2 = 1.8 \times 10^{-5} \text{ MeV}^{-2}$, however, if we take a large current quark mass $m = 130 \text{ MeV}$, the spin polarization occurs around $\mu \sim 845 \text{ MeV}$. Even if the coupling constant G_2 is small, the spin polarization is possible at high μ when the current quark mass is large.

Lastly, we shall comment on the case of large G_2 . Using the current quark mass $m = 5 \text{ MeV}$, we also carried out the numerical calculation with large $G_2 = 12 \times 10^{-5} \text{ MeV}^{-2}$. In this case, the region of μ where the spin polarization occurs becomes wide, and even at $\mu = 900 \text{ MeV} (= \Lambda)$ the spin polarization takes place $U_A > 0$.

5 Conclusion

We studied the relation between the quark spin polarization and spontaneous chiral symmetry breaking at finite density by use of the NJL type model with the number of colors $N_c = 3$ and the number of flavors $N_f = 1$, which includes interactions in vector and axial-vector channel. The self consistent equations for chiral condensate $\langle \bar{\psi} \psi \rangle$, spin polarization $\langle \psi^\dagger \Sigma_z \psi \rangle$, and quark number density $\langle \bar{\psi} \gamma^0 \psi \rangle$ are derived respectively in the framework of the Hartree approximation (mean field approximation). These simultaneous equations are solved numerically with the current quark mass 5 MeV and the axial-vector coupling constant $G_2 = 7 \times 10^{-5} \text{ MeV}^{-2}$, as a result of which we find how the quark spin polarization occurs as the quark chemical potential μ is increased.

The spin polarization begins to occur at a certain value of the chemical potential, at which the dynamical quark mass is still a few hundred MeV. The reason why the spin polarization occurs are that the quark number density is finite and that the dynamical quark mass remains relatively large value about a few hundred MeV. If the effective mass of the quark is taken to be 5 MeV, the spin polarization does not take place. When one increases the chemical potential furthermore, the spin polarization becomes weaker and finally disappears, where the chiral symmetry is partially restored and the dynamical mass M is fairly reduced from its value in the vacuum state. The reason why the spin polarization disappears at the large chemical potential is that the dynamical quark mass is fairly reduced by restoring partially the chiral symmetry. The effects of the dynamical mass M on the spin polarization U_A are discussed above; conversely, what is the effect of the spin polarization on the dynamical mass? The numerical calculations show that, if the spin polarization occurs $U_A > 0$, it operates to lower the dynamical quark mass M which is generated by spontaneous chiral symmetry breaking.

In studying the quark spin polarization with the moderate density at which chiral

symmetry is partially broken spontaneously, it is necessary to consider the relation between the spin polarization and spontaneous chiral symmetry breaking [3]; the present paper attempts to investigate such issue. However, there remains several problems not discussed here, and we show below;

- It is necessary to make sure that the nontrivial solution U_A of the self consistent equations gives the minimum value of the thermodynamical potential.
- The effect of quark confinement is not considered, since the NJL model we use is an effective theory that does not confine quarks. Although the lattice QCD simulation demonstrates quark confinement, it is difficult to apply it to the system with finite density. The development of this field is anticipated.
- We need to study the case of $SU(2)$ or $SU(3)$ flavors in which the condition of charge neutrality is imposed.
- If the color superconductivity is considered, one needs to investigate the relationship among the spin polarization, spontaneous chiral symmetry breaking, and the color superconductivity.
- We have done the numerical calculations with $T = 0$. It would be interesting to study numerically the finite temperature case $T > 0$.

Acknowledgments

The author thanks the Yukawa Institute for Theoretical Physics at Kyoto University. Discussions during the YITP workshop YITP-W-05-09 on "Thermal Quantum Field Theories and Their Applications" were useful to complete this work.

Appendix

A The calculation of the propagator G_A .

The G_A , Eq.(8), is calculated as follows. Following the notation used in the textbook of Bjorken and Drell [16], we write

$$[\not{p} - M + U_A \gamma_5 \gamma^3] = \begin{pmatrix} p_0 - U_A \sigma_3 - M & -\mathbf{p} \cdot \boldsymbol{\sigma} \\ \mathbf{p} \cdot \boldsymbol{\sigma} & -p_0 + U_A \sigma_3 - M \end{pmatrix}. \quad (\text{A.1})$$

By the way, the inverse of the matrix

$$X = \begin{pmatrix} A & B \\ C & D \end{pmatrix}, \quad (\text{A.2})$$

can be obtained by[17]

$$X^{-1} = \begin{pmatrix} -C^{-1}DU & Y \\ U & -B^{-1}AY \end{pmatrix}, \quad (\text{A.3})$$

where

$$\begin{aligned} U &\equiv (B - AC^{-1}D)^{-1}, \\ Y &\equiv (C - DB^{-1}A)^{-1}, \end{aligned} \quad (\text{A.4})$$

provided B^{-1} and C^{-1} exist. Using this formula, we get Eq.(8).

B Summation over the Matsubara frequency

Let us use the standard technique [14, 15] to calculate the sum $\sum_{j=-\infty}^{\infty}$ over the Matsubara frequency $\omega_j = (2j+1)\pi T$. Let $g(p^0)$ be a function of p^0 which decreases faster than $1/p^0$ for $|p_0| \rightarrow \infty$. Putting $p_0 = i\omega_j + \mu_r$, we obtain the following equation by the contour integration [15],

$$\frac{1}{\beta} \sum_{j=-\infty}^{\infty} g(p_0 = i\omega_j + \mu_r) = \sum \frac{\text{Res } g(p_0)}{e^{\beta(p_0 - \mu_r)} + 1}. \quad (\text{B.1})$$

Now, in Eq.(16), we take as follows

$$\begin{aligned} g(p_0) &= \frac{4 M(p^2 - M^2 + U_A^2)}{(p^2 - M^2 - U_A^2)^2 - 4 U_A^2 (M^2 + p_z^2)} \\ &= \frac{4 M(p^2 - M^2 + U_A^2)}{2(\epsilon_2^2 - \epsilon_1^2)} \sum_{n=1}^4 \frac{(-1)^n}{\epsilon_n} \frac{1}{(p_0 - \epsilon_n)}, \end{aligned} \quad (\text{B.2})$$

then Eq.(17) is derived by the formula Eq.(B.1).

C Explicit expressions for the self consistent equations

The self consistent equations Eq.(18), Eq.(20), and Eq.(24) with $T = 0$ can be calculated analytically when $0 \leq U_A < M$. The results are

$$\begin{aligned}
& M = m \\
& -G_1 \frac{N_c}{(2\pi)^2} M \left[\left\{ (\mu_r - 3U_A) \sqrt{(\mu_r - U_A)^2 - M^2} \right. \right. \\
& \quad + (2U_A(\mu_r - U_A) - M^2) \log \frac{(\mu_r - U_A) + \sqrt{(\mu_r - U_A)^2 - M^2}}{M} \left. \right\} \theta(\mu_r - (M + U_A)) \\
& \quad + \left\{ (\mu_r + 3U_A) \sqrt{(\mu_r + U_A)^2 - M^2} \right. \\
& \quad \left. \left. + (-2U_A(\mu_r + U_A) - M^2) \log \frac{(\mu_r + U_A) + \sqrt{(\mu_r + U_A)^2 - M^2}}{M} \right\} \theta(\mu_r - (M - U_A)) \right] \\
& + G_1 \frac{N_c}{(2\pi)^2} M \left[\mu_r \rightarrow \sqrt{\Lambda^2 + M^2} \right], \tag{C.1}
\end{aligned}$$

$$\begin{aligned}
& \mu_r = \mu \\
& -G_2 \frac{N_c}{(2\pi)^2} \left[\left\{ \frac{1}{3} \left(-2M^2 + (\mu_r - U_A)(2\mu_r + U_A) \right) \sqrt{(\mu_r - U_A)^2 - M^2} \right. \right. \\
& \quad \left. \left. - U_A M^2 \log \frac{(\mu_r - U_A) + \sqrt{(\mu_r - U_A)^2 - M^2}}{M} \right\} \theta(\mu_r - (M + U_A)) \right] \\
& -G_2 \frac{N_c}{(2\pi)^2} \left[U_A \rightarrow -U_A \right], \tag{C.2}
\end{aligned}$$

$$\begin{aligned}
U_A = & G_2 \frac{N_c}{(2\pi)^2} \left[\left\{ \frac{1}{3} \left(4M^2 - (\mu_r - U_A)(\mu_r + 2U_A) \right) \sqrt{(\mu_r - U_A)^2 - M^2} \right. \right. \\
& \quad \left. \left. - (\mu_r - 2U_A) M^2 \log \frac{(\mu_r - U_A) + \sqrt{(\mu_r - U_A)^2 - M^2}}{M} \right\} \theta(\mu_r - (M + U_A)) \right] \\
& -G_2 \frac{N_c}{(2\pi)^2} \left[U_A \rightarrow -U_A \right]. \tag{C.3}
\end{aligned}$$

References

- [1] I. Vidaña, A. Polls, and A. Ramos, Phys. Rev. C65, 035804 (2002); I. Vidaña and I. Bombaci, Phys. Rev. C66, 045801 (2002), and references therein.
- [2] T. Tatsumi, Phys. Lett. B489, 280 (2000); A. Niegawa, Prog. Theor. Phys. 113, 581 (2005).
- [3] E. Nakano, T. Maruyama, and T. Tatsumi, Phys. Rev. D68, 105001 (2003); T. Tatsumi, T. Maruyama, and E. Nakano, Prog. Theor. Phys. Suppl. 153, 190 (2004).
- [4] T. Maruyama and T. Tatsumi, Nucl. Phys. A693, 710 (2001).
- [5] For a review, see M. Buballa, Phys. Rep. 407, 205 (2005).
- [6] B.C. Barrois, Nucl. Phys. B129, 390 (1977).
- [7] D. Bailin and A. Love, Phys. Rep. 107, 325 (1984).
- [8] M. Asakawa and K. Yazaki, Nucl. Phys. A504, 668 (1989).
- [9] For a review, see S. P. Klevansky, Rev. Mod. Phys. 64, 649 (1992).
- [10] For example, M. Huang, hep-ph/0409167.
- [11] Y. Nambu and G. Jona-Lasinio, Phys. Rev. 122, 345 (1961).
- [12] M. Takizawa, K. Tsushima, Y. Kohyama, and K. Kubodera, Nucl. Phys. A507, 611 (1990).
- [13] S. Klimt, M. Lutz, U. Vogl, and W. Weise, Nucl. Phys. A516, 429 (1990).
- [14] J. I. Kapusta, *Finite-Temperature Field Theory* (Cambridge University Press, Cambridge, England, 1989).
- [15] M. LeBellac, *Thermal Field Theory* (Cambridge University Press, Cambridge, England, 1996).
- [16] J. D. Bjorken and S. D. Drell, *Relativistic Quantum Fields* (McGraw-Hill Book Co., New York, 1965).
- [17] J. Wess and J. Bagger, *Supersymmetry and Supergravity* (Princeton University Press, Princeton, 1992).